Glycerol metabolism of *Pichia pastoris* (*Komagataella spp.*) characterised by ^{13}C-based metabolic flux analysis

Màrius Tomàs-Gamisans[1], Anders Sebastian Rosenkrans Ødum[2], Mhairi Workman[4], Pau Ferrer[1,3], Joan Albiol[1]*

[1]Department of Chemical, Biological and Environmental Engineering, Universitat Autònoma de Barcelona, Bellaterra (Cerdanyola del Vallès), Catalonia, Spain

[2] Department of Biotechnology and Biomedicine, Technical University of Denmark, Lyngby, Denmark

[3] Current affiliation: Luxembourg Institute of Science and Technology, Luxembourg

[4] Novo Nordisk, Denmark.

*Corresponding author

Running title: ^{13}C-MFA of *P. pastoris* growing on glycerol

Abstract

Metabolic flux analysis based on ^{13}C-derived constraints has proved to be a powerful tool for quantitative physiological characterisation of one of the most extensively used microbial cell factory platforms, *Pichia pastoris* (syn. *Komagataella* spp.). Nonetheless, the reduced number of carbon atoms and the symmetry of the glycerol molecule has hampered the comprehensive determination of metabolic fluxes when used as labelled C-source. Moreover, metabolic models typically used for ^{13}C-based flux balance analysis may be incomplete or misrepresent the actual metabolic network. To circumvent these limitations, we reduced the genome-scale metabolic model iMT1026-v3.0 into a core model and used it for the iterative fitting of metabolic fluxes to the measured mass isotope distribution of proteinogenic amino acids obtained after fractional ^{13}C labelling of cells with [1,3-^{13}C]-glycerol. This workflow allows obtaining reliable estimates of *in vivo* fluxes in *P. pastoris* cells growing on glycerol as sole carbon source, as well as revising previous assumptions concerning its metabolic operation such as alternative metabolic branches, calculation of energetic parameters and proposed specific cofactor utilisation.

Keywords: ^{13}C-based metabolic flux analysis, *Pichia pastoris*, *Komagataella* spp, glycerol, genome-scale metabolic model

Introduction

Glycerol is a side stream in conventional biodiesel production processes and, therefore, its valorisation is a highly interesting option in the development of a glycerol-based integrated biorefinery concept [1,2]. Glycerol is an attractive feedstock to produce high value added compounds using microbial fermentation processes [3–

5]. Furthermore, the reduction degree of glycerol (4.67) is higher from that of glucose (4.0), and therefore higher yields of certain metabolites can be obtained from this compound [6]. However, crude glycerol typically contains several impurities such as methanol [7], which is toxic for most microbes with the exception of methylotrophic microorganisms. Notably, *P. pastoris* is able to efficiently use glycerol and/or methanol as energy and carbon sources [8–10]. In fact, the conventional promoters used for heterologous gene expression in this yeast (namely, P_{GAP}, constitutive, and P_{AOX}, inducible) have been isolated from genes related to glycerol and methanol metabolism [11,12]. Indeed, *P. pastoris* has been proven to grow on media containing crude glycerol [13,14], and does not need to be genetically engineered for improved glycerol utilisation, as done in other species like *S. cerevisiae*, [15–17], due to a more efficient glycerol transport system [16].Taken together, these attributes make *P. pastoris* a cell factory of high potential for the development of glycerol biorefineries.

However, there are very few systematic studies characterising growth of *P. pastoris* on glycerol as a sole carbon source [18,19]. Early ^{13}C-labelling experiments (CLE) performed with *P. pastoris* using glucose or glycerol as sole carbon sources were based on biosynthetically directed fractional (BDF) ^{13}C-labeling of proteinogenic amino acids with 2D-NMR, enabling the determination of metabolic flux ratios (METAFoR) [20]. This methodology relies on the identification of conserved C-C bounds in proteinogenic amino acids after feeding cells with a mixture of unlabelled and ^{13}C-uniformly labelled glucose as substrate [21,22]. However, the information derived using this technique when using labelled substrates with a low number of carbons such as glycerol, limits its application [18,20]. In addition, ^{13}C-based metabolic flux studies reported so far typically rely on metabolic models based on the pre-existing knowledge on

64 biochemical pathways of the central carbon metabolism, including the amino acid
65 biosynthesis pathways [18]. Such models have been extensively used, with just minor
66 modifications based on direct experimental observations, such as that glyoxylate
67 pathway or malic enzyme are not operative under the studied/similar growth
68 conditions [8], to improve metabolic flux determination using the available
69 experimental ^{13}C datasets [9,23–25].
70 Nevertheless, building such models by just combining well-known classical pathways
71 may easily result in a derived model with missing steps or pathways relevant for the
72 experimental conditions under study. As the ^{13}C based method for metabolic flux
73 determination does not include the cofactor balances (typically NAD(H)/NADP(H)),
74 verification of those balances after the metabolic fluxes have been determined may
75 reveal those inconsistencies in the underlying model. One way to overcome such
76 inconvenience could be the use of a genome-scale metabolic model (GSMM).
77 A genome-scale description of the *P. pastoris* metabolism has been developed over
78 different versions such as the iMT1026 GSMM [26], which was subsequently adapted
79 for growth on glycerol and methanol [19]. A priori, this GSMM would be an alternative
80 of choice for ^{13}C-MFA, due to its inclusion of a more complete number of pathways.
81 Nevertheless, large-scale ^{13}C-MFA has significant limitations such as the requirement
82 for an accurate and complete atom transition mapping. Although there are databases
83 including the reaction atom mapping of biological pathways, GSMM-specific reactions
84 would require the additional effort to accurately annotate atom transitions. Another
85 important hindrance for genome-scale ^{13}C-MFA is the resulting huge number of
86 variables that significantly impact computational complexity and performance, as well
87 as the difficulty or even impossibility in resolving all fluxes due to the robustness and

redundancy of metabolic pathways, which include parallel and alternative pathways and cell compartmentalization [27]. Due to this, nowadays GSMMs are still not a practical alternative to core metabolic models. Indeed, Gopalakrishnan and Maranas [28] have concluded that reducing GSMMs down to a size similar to the currently used core metabolism models used in ^{13}C-MFA would be a feasible alternative to the use of full GSMMs. In this regard, several algorithms for reducing GSMMs to core models have been developed. One method that appears particularly suited to our purpose is NetworkReducer [29], which allows to take into account the information derived from previous ^{13}C studies, such as the network topology -pathways proven to be active- in the tested experimental conditions. Briefly, this is achieved by protecting relevant reactions and applying phenotypic constrains while the algorithm successively eliminates or combines reactions until a minimal model that fulfils all the phenotypic constrains is obtained. This method has been recently employed in *E. coli* to produce a new core model (EColiCore2) producing flux distributions equivalent to those generated by the original GSMM [30].

In this study, the genome-scale metabolic model iMT1026 v3.0 [19] is reduced to a glycerol-specific core model. This reduced model is further used for ^{13}C-MFA of *P. pastoris* growing on glycerol as carbon source at different growth rates. In order to circumvent the limitation of using a 3C-substrate, a 1- and 3-positionally labelled glycerol is used, instead of a uniformly labelled substrate, together with the measurement of proteinogenic amino acids content and subsequent iterative fitting of metabolic fluxes to the measured mass isotope distribution (MIDs). Although this method does not allow the level of resolution achieved in non-stationary CLE, we show that such approach allowed us to improve the accuracy of the resolved fluxes in

112 comparison previous metabolic flux profiling studies based on METAFoR analysis
113 datasets.
114
115 **Materials and Methods**

116 ### Strain and cultivation conditions

117 The *Pichia pastoris* X-33 strain (Invitrogen-Thermofisher, Carlsbad, CA, USA) was used
118 throughout this study. Duplicate carbon-limited chemostat cultivations were
119 performed using a Sartorius 0.5-L bioreactor (Sartorius AG, Göttingen, Germany) at
120 dilution rates (D) of 0.05, 0.10 and 0.16 h^{-1} with a working volume of 0.3 L maintained
121 by a gravimetrically controlled peristaltic pump. Chemostat cultivations were
122 performed for at least 5 residence times (τ) prior to labelling.
123 Batch and chemostat media were adapted from Baumann *et al*. [31] by reducing
124 carbon and nitrogen sources concentrations for yielding an approximate final biomass
125 6 g/L when the steady state is reached. Thus, briefly, batch medium contained: 9.98
126 g/L glycerol, 0.46 g/L citric acid, 3.15 g/L $(NH_4)_2HPO_4$, 0.006 g/L $CaCl_2{\cdot}2H_2O$, 0.225 g/L
127 KCl, 0.125 g/L $MgSO_4{\cdot}7H_2O$, 0.5 mL Biotin (0.2 g/L), 1.15 mL PTM1 trace salts stock
128 solution (prepared as described in [31]). pH was adjusted to 5.0 with 25% HCl.
129 Chemostat medium contained: 10 g/L glycerol, 0.818 g/L citric acid, 4.35 g/L
130 $(NH_4)_2HPO_4$, 0.01 g/L $CaCl_2{\cdot}2H_2O$, 1.7 g/L KCl, 0.65 g/L $MgSO_4{\cdot}7H_2O$, 1.0 mL Biotin (0.2
131 g/L), 1.6 mL PTM1 trace salts stock solution and 0.2 mL/L of antifoam glanapon 2000
132 (Konc, Bussetti, Vienna, Austria).
133 An inoculum was cultivated overnight at 30°C, 150 rpm in a 0.5-L shake flask
134 containing 75 mL of basal medium with glycerol and supplemented with biotin (1%
135 yeast nitrogen base, $4 \cdot 10^{-5}$ % biotin, 1% glycerol). Bioreactor was inoculated an initial

OD_{600} of 0.3 – 0.5. Once glycerol was exhausted, continuous cultivations were started at the corresponding flow rate. The aeration rate was 1 vvm and the off-gas O_2 and CO_2 concentrations were measured using a Prima Pro Process Mass Spectrometer (Thermo Fischer Scientific). Temperature was maintained at 25°C. Stirring rate was 500 rpm and a pH 5.0 was controlled by automatic addition of 15% ammonia.

Labelling experiment and biomass harvest

After a minimum of 5τ of continuous cultivations with non-labelled glycerol, the feed was switched to the labelled medium. Labelled feed medium composition was the same as the unlabeled feed medium composition, replacing glycerol for 20% [1,3-^{13}C]-glycerol (CortecNet) and 80% unlabeled glycerol. Labelled medium was feed for at least 2τ. Culture samples (50 – 100 mL) were collected, centrifuged (15 min, 16000g), the supernatant discarded and pellets frozen with liquid N_2 and stored at -80°C for further extraction and analysis of proteinogenic amino acids.

Biomass and exometabolite analysis

Cell density and dry cell weight

Cell density was monitored by optical density at 600 nm. Dry cell weight (DCW) was measured in duplicate by gravimetric methods. Briefly, a known volume of sample (5 to 10 mL) was filtered throughout a dried pre-weighted 0.45 µm polyether sulfone filters (Frisenette, Knebel, Denmark) and washed with distilled water. Filters were dried in a microwave oven at 150 W for 20 min and cooled down in a desiccator for at least 2 h and finally weighted.

Exometabolite analysis

158 Samples taken for external metabolite analysis, were filtered through a 0.22 µm
159 syringe filters and stored at -20°C until subsequent analysis. Glycerol, was the only
160 peak detected in HPLC analyses performed as described in [32].

161 Proteinogenic amino acid MID determination

162 Amino acid extraction, derivatization and GC-MS analysis

163 Isotope distribution of the proteinogenic amino acid (MID) was determined as
164 described by Knudsen [33]. Briefly, 5 mg of biomass pellets were hydrolyzed with 6 M
165 hydrochloric acid at 105°C for 16 h. Once at room temperature, samples were dried for
166 3h under a stream of nitrogen. Samples were redissolved in water and filtered through
167 Strata SCX (100 mg, 1 cc, Phenomenex, Torrance, CA, USA) columns and washed with
168 50% ethanol to remove all the impurities. Samples were eluted with 1 N NaOH and
169 additionally with the elution solution [33]. Two types of derivatives were prepared for
170 GC-MS analysis: N-ethoxycarbonyl-amino ethyl-esters (ECF) and N-dimethyl-amino-
171 methylene-methyl-esters (DMFDMA) following the accurate protocol described by
172 Knudsen [33]. Derivatized amino acid samples were analyzed in a GC-MS Agilent 6890
173 gas chromatograph coupled to an Agilent 5973 quadruple MS accordingly to the
174 specified settings [33]. GC/MS Translator (Agilent) was used to convert the resulting
175 row data files into readable for Agilent MassHunter Qualitative Analysis software.

176 MID correction for natural isotopes and washout kinetics

177 MID are uncorrected for naturally labelled atoms other than carbon backbone [34,35].
178 OpenFlux [36] was used for correcting the MID of each amino acid according to the
179 expected fragmentation ions obtained in GC-MS analysis [37]. In addition, biomass was
180 harvested at 2 τ after the onset of labelling and thus, the fraction of labelled biomass

($X_{labelled}$) at the steady state was calculated according to a first-order wash-out kinetics [18]: $X_{labelled} = 1 - e^{-t/\tau}$, where t is the labelling time and τ the residence time of the chemostat. Corrected MIDs for each experimental replicate and corresponding analysed peaks from each corresponding derivatisation method can be found in additional file S2, Table S2.

Statistical analysis

Chemostat cultivation data was checked for consistency using elemental mass balances and common reconciliation procedures [38]. The biomass molecular formula used was selected according to the specific biomass composition of *P. pastoris* growing on glycerol [19]. In all the cultivation sets, statistical consistency test was passed with a confidence level of 95%. Consequently, there was no evidence of gross measurement errors.

Core model generation

In order to obtain a representative network of the central carbon metabolism of *P. pastoris*, including all the relevant reactions a core model (*PpaCore*) was derived from iMT1026 v3.0 model using NetworkReducer [29] with CellNetAnalyser 2016.1 [39] under Matlab 2011. A detailed procedure and commands for model reduction can be found in additional File S1. Default flux constrains for glycerol growth as the only possible carbon source were set. Maximal growth rate in the reduced network is constrained to be 99.9% of the maximal growth rate for the iMT1026 v3.0 (here *PpaGS*, meaning '*P. pastoris* Genome-Scale') corresponding to the glycerol chemostat cultivations in our previous work [19]. In a first step, 46 reactions of the central carbon metabolism were protected (additional File S1) and *PpaGS* was reduced to a pruned

model (*PpaPruned*). Subsequently, *PpaPruned* was further reduced to *PpaCore* by a compressing procedure with a new set of 56 protected reactions (additional File S1). Due to numerical reasons the 'cof' metabolite was removed from biomass equation. The resulting *PpaCore* was tested for growth in glycerol and the same maximal growth rates obtained in *PpaGS* were achieved for a constrained uptake of glycerol.

^{13}C-Metabolic flux analysis (^{13}C-MFA)

Flux calculations were performed with OpenFLUX [36] under Matlab 2011 using FMINCON from Matlab's optimization toolbox. Previously to perform MFA, *PpaCore* was adapted to OpenFLUX requirements in three steps: (1) each reversible reaction was replaced by two paired irreversible reactions; (2) reactions mapping label distribution in the measured proteinogenic amino acids were added according to the appropriate compartmentalization [20]; (3) carbon atom transition equations were added according to previous *P. pastoris* models [9] and databases [40]. In order to avoid biased solutions, O_2, reduction equivalents, energetic cofactors and additional non-carbon-balanceable metabolites were defined as excluded metabolites. Moreover, those reactions in *PpaCore* that uniquely contained excluded metabolites were also removed from the final model for ^{13}C-metabolic flux calculations. The resulting model (additional File S2 Table S1) was used for ^{13}C-MFA. Experimental MIDs showed an average deviation below 5% and the model was fitted to the experimental data by the least squares method detailed in [41] using the measured glycerol uptake rate and specific biomass generation rates as constrains. The parameter estimation procedure was repeated 100 times. Subsequently, the solution cluster with lower residual error was used for sensitivity analysis using the non-linear approach of Antoniewicz [42]. Sensitivity analysis was performed in order to find the lower and upper confidence

interval boundaries of calculated fluxes at a 95% confidence level [36]. Default configuration settings were used for the sensitivity analysis. In those cases, where it was impossible to determine individually the forward and reverse fluxes, only the net fluxes were calculated and subjected to sensitivity analysis. Flux fitting to ^{13}C MID was performed individually for each experimental replicate and subsequently averaged. Main results were depicted using Omix graphic software [43].

Calculation of redox cofactor regeneration rates and energy requirements

Rates for redox cofactor regeneration and ATP synthesis were derived after calculation of the other fluxes. Once the solution of the metabolic system was found, estimated fluxes were further used for calculating the remaining reaction fluxes that contained excluded metabolites. Redox cofactor balance was checked and any surplus of reduction equivalents (NADH both cytosolic and mitochondrial) was considered a source of electrons transferred to the electron transport chain (ECT). Therefore, assuming the complete electron transfer from the surplus reduction equivalents to ETC and taking into account the oxygen requirements for biomass synthesis (included in the full biomass equation), the oxygen uptake rate could be calculated and compared to the experimental values. In addition, since the model includes the complete ETC with proton translocation to the mitochondrial intermembrane space and the corresponding reaction for ATP synthesis [26], a theoretical maximal ATP generation rate can be estimated. The total ATP generation was taken later into account for calculating the energetic parameters. Essentially, two parameters were determined: growth and non-growth associated maintenance energy (GAME and NGAME, respectively) according to Pirt's equation [44] and applying a linear regression between ATP generation and growth rates [45]. The y-intercept would correspond to the

NGAME (μ = 0.0 h^{-1}) and the slope to GAME (Fig. S1). Those values can be later compared to those obtained using the complete *PpaGS* model.

Results and discussion

Macroscopic growth parameter characterisation

Despite the increasing interest on using glycerol as feedstock for microbial biorefineries, there is limited information on the physiology of *P. pastoris* growing on such carbon source. In a recent study [19], we performed a series of cultivations at different growth rates using glycerol as sole carbon source. These data allowed to analyse the effects of growth rate on biomass composition in a comprehensive way.

In this study, a new series of carbon-limited chemostat cultivations using glycerol as sole carbon source has been performed at three different dilution rates (corresponding to a low, mid and high ranges) that had been already previously tested [19,20], namely: 0.05, 0.10 and 0.16 h^{-1}. In order to obtain equivalent datasets, the culture medium composition was the same as in our recent study, except for glycerol concentration in the feed medium, which was reduced to obtain a lower steady state biomass concentration.

In agreement with our previous experiments, *P. pastoris* cells growing under these conditions showed no by-product secretion and residual glycerol in the broth samples was below the detection limit of the analytical method. All the measured external macroscopic fluxes showed a clear correlation with the growth rate (R^2 > 0.99), consistent with our previous study [19], where a linear range for the cell's macroscopic variables when growing on glycerol was established between 0.05 and 0.16 h^{-1} growth rate. Biomass yields (Y_{XS}) ranged between 0.70 – 0.72 $g_X \cdot g_S^{-1}$ (Table 1). These values are in the upper range of Y_{XS} previously reported for glycerol as C-source [19] and are

276 also in agreement with biomass yields on glycerol reported for other yeast species
277 [46]. Similarly, the average experimental RQ (0.58 $\pm$ 0.02) was close to 0.63 $\pm$ 0.03, the
278 average RQ experimentally determined in our previous study for glycerol-grown cells.
279 Therefore, despite reducing the carbon source concentration in the feed medium, cells
280 showed comparable macroscopic profiles and therefore reflected comparable
281 cultivations conditions.

282 ## Reduction of *P. pastoris* genome-scale model

283 The iMT1026 v3.0 model was used for deriving central carbon metabolism model
284 in two reduction steps, generating *PpaPruned* and *PpaCore*. The main characteristics of
285 the reduced model are summarized in Table 2. In order to avoid infeasibilities due to
286 numerical tolerance constrains, 'cof' metabolite corresponding to cofactors in biomass
287 equation was removed. 'COF' reaction has stoichiometric coefficients of the order of
288 $1x10^{-6}$ that can be lower than the minimal calculation tolerance. By removing COF, no
289 significant impact on the flux distribution or the predictability capacity was observed.
290 In the first reduction step, the 46 reactions were protected. These reactions included
291 the equivalent reactions to the previous *P. pastoris* central carbon metabolism model
292 [24] as well as relevant transport reactions across cell compartments. Protected
293 phenotypes were stablished in order to ensure the accuracy of the predictions, i.e. the
294 99.9% of the maximal predicted growth rate in the original model for a given glycerol
295 uptake rate. As reported previously [19], no by-product generation was detected when
296 growing in glycerol-limited chemostats. None of the by-product formation reactions
297 were protected and consequently none of them were present in *PpaPruned* in
298 agreement with experimental data previously reported [19]. Initially, the genome scale
299 metabolic model contained 2237 reactions and 1881 metabolites (175 external). As a

result of the network reduction the number of reactions and metabolites was considerably reduced (495 reactions and 513 metabolites). The degrees of freedom (*dof*) were also strongly reduced (from 485 to 4). This reduction could be due to the fact that the pruned model only considers growth on glycerol with no by-product generation. In the subsequent step, *PpaPruned* was further reduced by applying a loss-free network compression step [29], where mainly consecutive, parallel and transport reactions were lumped. As a result, *PpaCore* was generated including 77 reactions with 102 metabolites with no further reduction in degrees of freedom. The maximal predicted growth rate was identical as the one obtained with the original model.

^{13}C-Metabolic flux analysis of glycerol-grown cells

The generated model was implemented in OpenFLUX code for ^{13}C-MFA determination as described above (Table S1). Flux values are presented in **Error! No s'ha trobat l'origen de la referència.** as the 95% confidence interval (CI) in order to provide a more informative description of the results taking into account the uncertainty of estimated fluxes [42]. Although flux values expressed as mean of the optimal value ± SEM would provide an overview of changes in the estimated fluxes, this would not indicate the real uncertainty of the measurement due to the asymmetry of the interval. Then, in this study metabolic fluxes are expressed as confidence interval boundaries.

To our knowledge, there is only one previous study analysing the metabolic flux distribution of glycerol-grown yeasts based on ^{13}C-labelling experiments [20] using metabolic flux ratio analysis (METAFoR) and thus absolute metabolic flux values were not provided. Moreover, such analysis was limited to the pyruvate node and tricarboxylic acid cycle (TCA) due to the limitations caused by the use of a 3-carbon source such as glycerol. Notably, the flux ratios derived from the metabolic flux

calculations performed in the present study are consistent with those obtained using METAFoR analysis. In particular, Solà *et al.* [20] reported a very low activity through glyoxylate cycle. This observation was based on the absence of carbon labelling patterns compatible with the activity of this pathway, also supported by previous studies in *S. cerevisiae* and *P. stipitis* [47]. In addition, Solà *et al*. [20] measured the activity of isocitrate lyase (ICL), showing basal levels in both glucose- and glycerol-grown *P. pastoris* chemostats. Since glucose is known to repress the glyoxylate pathway in *S. cerevisiae* [48] and measured activities of ICL in *P. pastoris* were similar for glucose and glycerol, it was concluded that the flux through glyoxylate cycle was negligible. This consideration has also been subsequently assumed in later studies [24,49–52] by omitting the glyoxylate pathway from the metabolic network for ^{13}C-MFA. As shown in **Error! No s'ha trobat l'origen de la referència.**, the activity through glyoxylate cycle found in the present study is very low, almost negligible, and thus confirms the previous assumptions by Solà *et al*. [20]. A second observation by Solà and co-workers was that the fraction of mitochondrial pyruvate derived from malate was also very low or negligible, thus indicating that the malic enzyme is likewise almost inactive in cells growing on glycerol-limited chemostats. Our calculations are in agreement with this observation. However, for the lowest dilution rate tested (0.05 h^{-1}), the relative flux through the malic enzyme reaction appears to be higher than at the other dilution rates. Nevertheless, this flux is less than 20% of the carbon flux contribution to the mitochondrial pyruvate pool.

The flux split ratio between gluconeogenesis and pentose phosphate pathway cannot be assessed when using biosynthetically directed fractional ^{13}C labelling of proteinogenic amino acids based on uniformly labelled glycerol or glycerol/methanol

348 mixtures [8,20]. Nevertheless, when applying the global fitting approach, fluxes
349 through the oxidative branch of the pentose phosphate pathway (PPP) have been
350 estimated for cells growing under such conditions [9]. Coherently with these previous
351 studies [9], our results indicate that the flux through the oxidative branch of PPP is
352 almost negligible (**Error! No s'ha trobat l'origen de la referència.**). Thus, the majority
353 of NADPH generated in cytosol would be produced in other reactions, such as the
354 glycerol oxidation. Flux directionality in non-oxidative branch of PPP could only be
355 determined within the 95% CI for cells growing at D = 0.05 h^{-1}. In the other two
356 conditions tested, estimated CI includes both reaction directions as feasible **Error! No**
357 **s'ha trobat l'origen de la referència.**. This uncertainty on estimated PPP fluxes has
358 been previously described and attributed to the operation of PPP reactions close to
359 the thermodynamic equilibrium, i.e. bidirectionally feasible [53].
360 The resulting core model included several mitochondrial transporters that also act as
361 redox shuttles [54]. Nevertheless, the malate/aspartate shuttle appears to be the
362 major redox shuttle and TCA cycle intermediate metabolite transporter **Error! No s'ha**
363 **trobat l'origen de la referència.**, while the flux through other transporters was
364 estimated to be very low, almost negligible. High exchange rates of
365 mitochondrial/cytosolic oxaloacetate were observed in previous studies on glycerol
366 [20]. Authors suggested the existence of a highly active mitochondrial shuttle.
367 Moreover, in cultivations on mixtures of glycerol and methanol, a high transcription of
368 genes involved in the malate/aspartate shuttle was reported [25]. Therefore, those
369 previous studies support our results that point at the malate/aspartate shuttle as the
370 major redox shuttle and TCA cycle intermediate metabolites transporter.

Impact of dilution rate on metabolic flux distribution

Although the flux through the oxidative branch of PPP is very low, and could therefore be considered as negligible, the upper bound of the CI of the relative flux through the oxidative part of PPP appears to increase with the growth rate while the uncertainty in the measured data is similar. Hence, while cultivations at 0.05 h^{-1} are estimated to have a relative flux between 0 and 0.2, those at 0.10 and 0.16 h^{-1} showed a CI upper bound of 6.7 and 13.9 respectively. Thus, it would suggest that at higher growth rates, the average relative flux through the oxidative branch of PPP is in fact higher than at lower growth rates. Consequently, the upper bounds for the non-oxidative part of the PPP are also increased at higher growth rates. As recently detailed for *P. pastoris* [19], the growth rate hypothesis (GRH) describes a positive correlation between the growth rate and the RNA and protein content [55–57]. Moreover, the analysis performed of the RNA content of cells growing on glycerol at different growth rates also depicts this positive correlation [19]. Considering that major precursors for nucleic acids biosynthesis are generated in the pentose phosphate pathway [45], an additional demand of RNA would require an increase in PPP activity. Thus, the estimated increase in relative flux through the oxidative branch of PPP at high growth rates is consistent with the additional demand for RNA precursors, in agreement with the GRH recently described for *P. pastoris* [19]. Concomitantly, the split ratio between gluconeogenesis-PPP and lower glycolysis at the glyceraldehyde 3-phosphate node is also altered with the growth rate. As a result of the increase in the relative flux though gluconeogenesis and PPP at higher growth rates, there is a reduction of relative flux through the lower glycolysis part and consequently to the TCA cycle (**Fig. 1**). Similar results were reported by Jordà *et al*. [9] in chemostat cultivations using mixtures of glycerol and methanol as

carbon sources at low and high dilution rates (0.05 and 0.16 h^{-1}). Among the different mixtures of glycerol and methanol tested, a qualitative comparison of our results with the reported condition at lower methanol:glycerol ratio (20:80, w/w) can be performed. In this study, invariant absolute fluxes through the TCA cycle (citrate synthase reaction) were observed when comparing low and high growth rates, while the substrate uptake rate was much higher at the highest growth rate. Therefore, the flux through citrate synthase reaction relative to the substrate uptake rate was significantly reduced at the high growth rate, in agreement with the present results.

A correlation with the relative flux through the malate/α-ketoglutarate transporter and the growth rate is also observed. The upper bound of the CI increases with the dilution rate, thus the relative flux for D=0.16 h^{-1} would be the highest possible with respect to the other conditions. These results are also in agreement with those described by Solà *et al*. [20]. There, authors described that at higher growth rates the cytosolic-mitochondrial exchange flux of oxaloacetate was largely unidirectional from the cytosol to the mitochondria. A flux increase in malate/α-ketoglutarate exchange reaction is coherent with the increased unidirectional transport of oxaloacetate into the mitochondria, previously observed under similar growth conditions [20], as malate is subsequently oxidised to oxaloacetate in this organelle. That is, a flux increase in the malate/α-ketoglutarate shuttle could in fact reflect an increase of the oxaloacetate transport net flux into the mitochondria.

Redox cofactor regeneration and energy metabolism

Redox cofactors were excluded from the metabolic flux calculation step using carbon labelling data in order to avoid biased solutions. Consequently, metabolic fluxes are

418 derived exclusively from the adjustment of experimental MIDs to the calculated
419 metabolic isotope distribution and measured input/output fluxes with no interference
420 of other additional information. Once the metabolic fluxes were estimated, a
421 calculation of both oxygen and cofactor regeneration was performed in order to check
422 whether the estimated solution implicitly satisfies the electron balance. Initially, the
423 estimated flux distribution solution predicted an excess of cytosolic NADH that could
424 not be oxidised. Cells have redox shuttles that are able to transport NADH indirectly
425 from cytosol to mitochondria [54]. One of these redox shuttles is the malate-aspartate
426 shuttle. In this particular case, despite being present in *PpaCore*, the exact specific
427 activity of the mitochondrial shuttle cannot be calculated as no carbon rearrangement
428 takes place. Consequently, only the net flux in the shuttle system can be calculated
429 (i.e. difference between the cytosolic and mitochondrial flux). Therefore, scaled fluxes
430 in both compartments would result in identical flux relative distributions, but with
431 additional amounts of NADH being translocated to the mitochondria. Regarding the
432 inability to predict scaled up fluxes in redox shuttles employing the currently used
433 constrains, an additional flux fitting was performed by adding the cytosolic NAD(H)
434 balance to the stoichiometric matrix for flux estimation. As a result, identical flux
435 distributions were obtained for reactions other than the mitochondrial redox shuttle.
436 Moreover, the increase in flux of mitochondrial redox shuttle in the new calculation
437 corresponds exactly to the calculated excess of cytosolic NADH. Correspondingly, the
438 theoretical oxygen consumption rates were calculated assuming that all the NADH
439 excess is consumed in the ETC. Oxygen requirements included in the biomass equation
440 were also taken into account and constrained in the ETC calculations. Thus, for each
441 growth rate, the theoretically calculated oxygen requirements account for over 97% of

442 the experimentally determined oxygen consumption rates. Therefore, metabolic fluxes
443 and calculated variables are highly consistent with the experimental data.
444 Using the metabolic flux distributions and a global electron balance, maximal ATP
445 generation rates were also calculated. Thus, growth associated and non-associated
446 maintenance energy was calculated as described in the Materials and Methods
447 section. The y-intersection in the regression of maximal ATP generation rates with the
448 growth rate is 1.22 ± 0.48 mmol ATP · g_{DCW}^{-1} · h^{-1} and corresponds to the NGAME (See
449 Fig. S1 for the graphical representation). Despite the difference, this value is
450 comparable with the 2.51 reported in our previous study [19] for cultivations on
451 glycerol. In addition, GAME was estimated to be 88.8 ± 4.1 mmol ATP · g_{DCW}^{-1}, that is
452 higher but comparable to the 70.7 mmol ATP · g_{DCW}^{-1} calculated in the previous study,
453 given that only 3 different growth rates are available.
454 It is worth mentioning that the oxidative branch of PPP is usually considered the
455 major source of cytosolic NADPH [49,58]. Nevertheless, the predicted flux through this
456 pathway in this case is very low, almost negligible, in accordance with previous ^{13}C-
457 MFA estimations on mixtures of glycerol and methanol [9]. In fact, those studies
458 already suggested that alternative reactions must supply the required cytosolic
459 NADPH, otherwise a NADPH imbalance was observed. Our GSMM contains all the
460 relevant reactions producing NADPH in cytosol. As a result of automatic model
461 reduction, *PpaCore* contained the $NADP^+$-dependent glycerol oxidation, although
462 previous core models proposed a NAD^+-dependent glycerol oxidation. Therefore, it
463 seems plausible that the $NADP^+$-dependent oxidation of glycerol pathway is used in
464 glycerol-grown cells. In this way, it would be the major source for cytosolic NADPH
465 formation.

Conclusions

The use of ^{13}C-positionally labelled glycerol in the steady state CLEs combined with the analysis of the labelling patterns of proteinogenic amino acids allowed, for the first time, a more reliable estimation of metabolic fluxes through the central carbon pathways of *P. pastoris* cells growing on glycerol as sole C-source within an acceptable confidence range. A new protocol was used to determine the metabolic flux distributions of *P. pastoris* growing in glycerol at different dilution rates. The results allowed to verify previous hypothesis, calculate energetic parameters and propose alternative cofactor utilization.

Furthermore, we have developed and tested a more robust steady state workflow for ^{13}C-MFA of yeast growing on glycerol as sole carbon source, enabling efficient support for glycerol-based metabolic and bioprocess engineering applications.

Acknowledgements

This work was supported by the project CTQ2013- 42391-R and CTQ2016-74959-R (AEI/FEDER, UE) of the Spanish Ministry of Economy, Industry and Competitiveness, 2014-SGR-452 of the Reference Network in Biotechnology (XRB) (Generalitat de Catalunya) and the grant FPU FPU12/06185 (M.T.) of the Spanish Ministry of Education, Culture and Sport and the Short-Term Fellowship (M.T.) of the European Molecular Biology Organisation. In addition, the authors would like to acknowledge partial support from the ERA- IB IPCRES project.

References

[1] Kiss AA, Grievink J, Rito-Palomares M. A systems engineering perspective on process integration in industrial biotechnology. J Chem Technol Biotechnol 2015;90:349–55. doi:10.1002/jctb.4584.

[2] Chen Z, Liu D. Toward glycerol biorefinery: metabolic engineering for the production of biofuels and chemicals from glycerol. Biotechnol Biofuels 2016;9:205. doi:10.1186/s13068-016-0625-8.

[3] Valerio O, Horvath T, Pond C, Misra M, Mohanty A. Improved utilization of crude glycerol from biodiesel industries: Synthesis and characterization of sustainable biobased polyesters. Ind Crops Prod 2015;78:141–7. doi:10.1016/j.indcrop.2015.10.019.

[4] Johnson DT, Taconi KA. The glycerin glut: Options for the value-added conversion of crude glycerol resulting from biodiesel production. Environ Prog 2007;26:338–48. doi:10.1002/ep.10225.

[5] Yang F, Hanna M a, Sun R. Value-added uses for crude glycerol--a byproduct of biodiesel production. Biotechnol Biofuels 2012;5:1–10. doi:10.1186/1754-6834-5-13.

[6] da Silva GP, Mack M, Contiero J. Glycerol: A promising and abundant carbon source for industrial microbiology. Biotechnol Adv 2009;27:30–9. doi:10.1016/j.biotechadv.2008.07.006.

[7] Posada J a, Rincón LE, Cardona C a. Design and analysis of biorefineries based on raw glycerol: addressing the glycerol problem. Bioresour Technol 2012;111:282–93. doi:10.1016/j.biortech.2012.01.151.

[8] Solà A, Jouhten P, Maaheimo H, Sánchez-Ferrando F, Szyperski T, Ferrer P. Metabolic flux profiling of *Pichia pastoris* grown on glycerol/methanol mixtures in chemostat cultures at low and high dilution rates. Microbiology 2007;153:281–90. doi:10.1099/mic.0.29263-0.

[9] Jordà J, De Jesus SS, Peltier S, Ferrer P, Albiol J. Metabolic flux analysis of recombinant *Pichia pastoris* growing on different glycerol/methanol mixtures by iterative fitting of NMR-derived 13C-labelling data from proteinogenic amino acids. N Biotechnol 2014;31:120–32. doi:10.1016/j.nbt.2013.06.007.

[10] Çelik E, Ozbay N, Oktar N, Çalık P. Use of Biodiesel Byproduct Crude Glycerol as the Carbon Source for Fermentation Processes by Recombinant *Pichia pastoris*. Ind Eng Chem Res 2008;47:2985–90. doi:10.1021/ie071613o.

[11] Cos O, Ramón R, Montesinos JL, Valero F. Operational strategies, monitoring and control of heterologous protein production in the methylotrophic yeast *Pichia pastoris* under different promoters: a review. Microb Cell Fact 2006;5:17. doi:10.1186/1475-2859-5-17.

[12] Gasser B, Prielhofer R, Marx H, Maurer M, Nocon J, Steiger M, et al. *Pichia pastoris*: protein production host and model organism for biomedical research. Future Microbiol 2013;8:191–208. doi:10.2217/fmb.12.133.

[13] Anastácio GS, Santos KO, Suarez PAZ, Torres FAG, De Marco JL, Parachin NS. Utilization of glycerin byproduct derived from soybean oil biodiesel as a carbon source for heterologous protein production in *Pichia pastoris*. Bioresour Technol 2014;152:505–10. doi:10.1016/j.biortech.2013.11.042.

[14] Lopes M, Belo I, Mota M. Batch and fed-batch growth of *Pichia pastoris* under increased air pressure. Bioprocess Biosyst Eng 2013;36:1267–75. doi:10.1007/s00449-012-0871-5.

[15] Ho P-W, Swinnen S, Duitama J, Nevoigt E. The sole introduction of two single-point mutations establishes glycerol utilization in *Saccharomyces cerevisiae* CEN.PK derivatives. Biotechnol Biofuels 2017;10:10. doi:10.1186/s13068-016-0696-6.

[16] Klein M, Swinnen S, Thevelein JM, Nevoigt E. Glycerol metabolism and transport in yeast and fungi: established knowledge and ambiguities. Environ Microbiol 2017;19:878–93. doi:10.1111/1462-2920.13617.

[17] Klein M, Carrillo M, Xiberras J, Islam Z, Swinnen S, Nevoigt E. Towards the exploitation of glycerol's high reducing power in *Saccharomyces cerevisiae* -based bioprocesses. Metab Eng 2016;38:464–72. doi:10.1016/j.ymben.2016.10.008.

[18] Ferrer P, Albiol J. 13C-Based Metabolic Flux Analysis in Yeast: The *Pichia pastoris* Case. In: Mapelli V, editor. Methods Mol. Biol., vol. 1152, New York, NY: Springer New York; 2014, p. 209–32. doi:10.1007/978-1-4939-0563-8_13.

[19] Tomàs-Gamisans M, Ferrer P, Albiol J. Fine-tuning the *P. pastoris* iMT1026 genome-scale metabolic model for improved prediction of growth on methanol or glycerol as sole carbon sources. Microb Biotechnol 2018;11:224–37. doi:10.1111/1751-7915.12871.

[20] Solà A, Maaheimo H, Ylönen K, Ferrer P, Szyperski T. Amino acid biosynthesis and metabolic flux profiling of *Pichia pastoris*. Eur J Biochem 2004;271:2462–70. doi:10.1111/j.1432-1033.2004.04176.x.

[21] Maaheimo H, Fiaux J, Petek Çakar Z, Bailey JE, Sauer U, Szyperski T. Central carbon metabolism of *Saccharomyces cerevisiae* explored by biosynthetic fractional 13C labeling of common amino acids. Eur J Biochem 2001;268:2464–79. doi:10.1046/j.1432-1327.2001.02126.x.

[22] Szyperski T, Glaser RW, Hochuli M, Fiaux J, Sauer U, Bailey JE, et al. Bioreaction Network Topology and Metabolic Flux Ratio Analysis by Biosynthetic Fractional ^{13}C Labeling and Two-Dimensional NMR Spectroscopy. Metab Eng 1999;1:189–97. doi:10.1006/mben.1999.0116.

[23] Jordà J, Jouhten P, Cámara E, Maaheimo H, Albiol J, Ferrer P. Metabolic flux profiling of recombinant protein secreting *Pichia pastoris* growing on glucose:methanol mixtures. Microb Cell Fact 2012;11:57. doi:10.1186/1475-2859-11-57.

[24] Baumann K, Carnicer M, Dragosits M, Graf AB, Stadlmann J, Jouhten P, et al. A multi-level study of recombinant *Pichia pastoris* in different oxygen conditions. BMC Syst Biol 2010;4:141. doi:10.1186/1752-0509-4-141.

[25] Rußmayer H, Buchetics M, Gruber C, Valli M, Grillitsch K, Modarres G, et al. Systems-level organization of yeast methylotrophic lifestyle. BMC Biol 2015;13:80. doi:10.1186/s12915-015-0186-5.

[26] Tomàs-Gamisans M, Ferrer P, Albiol J. Integration and Validation of the Genome-Scale Metabolic Models of *Pichia pastoris*: A Comprehensive Update of Protein Glycosylation Pathways, Lipid and Energy Metabolism. PLoS One 2016;11(1):e0148031. doi:10.1371/journal.pone.0148031.

[27] Gopalakrishnan S, Maranas C. Achieving Metabolic Flux Analysis for *S. cerevisiae* at a Genome-Scale: Challenges, Requirements, and Considerations. Metabolites 2015;5:521–35. doi:10.3390/metabo5030521.

[28] Gopalakrishnan S, Maranas CD. 13C metabolic flux analysis at a genome-scale. Metab Eng 2015;32:12–22. doi:10.1016/j.ymben.2015.08.006.

[29] Erdrich P, Steuer R, Klamt S. An algorithm for the reduction of genome-scale metabolic network models to meaningful core models. BMC Syst Biol 2015;9:48. doi:10.1186/s12918-015-0191-x.

[30] Hädicke O, Klamt S. *EColiCore2*: a reference network model of the central metabolism of *Escherichia coli* and relationships to its genome-scale parent model. Sci Rep 2017;7:39647. doi:10.1038/srep39647.

[31] Baumann K, Maurer M, Dragosits M, Cos O, Ferrer P, Mattanovich D. Hypoxic fed-batch cultivation of *Pichia pastoris* increases specific and volumetric productivity of recombinant proteins. Biotechnol Bioeng 2008;100:177–83. doi:10.1002/bit.21763.

[32] Liu X, Mortensen UH, Workman M. Expression and functional studies of genes involved in transport and metabolism of glycerol in *Pachysolen tannophilus*. Microb Cell Fact 2013;12:27. doi:10.1186/1475-2859-12-27.

[33] Knudsen PB, Workman M, Nielsen KF, Thykaer J. Development of scalable high throughput fermentation approaches for physiological characterisation of yeast and filamentous fungi. Ph.D. Thesis. Kgs. Lyngby. Technical University of Denmark, 2015.

[34] Fernandez CA, Rosiers C Des, Previs SF, David F, Brunengraber H. Correction of ^{13}C Mass Isotopomer Distributions for Natural Stable Isotope Abundance. J Mass Spectrom 1996;31:255–62. doi:10.1002/(SICI)1096-9888(199603)31:3<255::AID-JMS290>3.0.CO;2-3.

[35] Van Winden WA, Wittmann C, Heinzle E, Heijnen JJ. Correcting mass isotopomer distributions for naturally occurring isotopes. Biotechnol Bioeng 2002;80:477–9. doi:10.1002/bit.10393.

[36] Quek L-E, Wittmann C, Nielsen LK, Krömer JO. OpenFLUX: efficient modelling software for 13C-based metabolic flux analysis. Microb Cell Fact 2009;8:25. doi:10.1186/1475-2859-8-25.

[37] Christensen B, Nielsen J. Isotopomer Analysis Using GC-MS. Metab Eng 1999;1:282–90. doi:10.1006/mben.1999.0117.

[38] Noorman HJ, Romein B, Luyben KC a M, Heijnen JJ. Classification, error detection, and reconciliation of process information in complex biochemical systems. Biotechnol Bioeng 2000;49:364–76. doi:10.1002/(SICI)1097-0290(19960220)49:4<364::AID-BIT2>3.0.CO;2-N.

[39] Klamt S, Saez-Rodriguez J, Gilles ED. Structural and functional analysis of cellular networks with *CellNetAnalyzer*. BMC Syst Biol 2007;1:2. doi:10.1186/1752-0509-1-2.

[40] Caspi R, Altman T, Billington R, Dreher K, Foerster H, Fulcher C a., et al. The MetaCyc database of metabolic pathways and enzymes and the BioCyc collection of Pathway/Genome Databases. Nucleic Acids Res 2014;42:459–71. doi:10.1093/nar/gkt1103.

[41] Antoniewicz MR, Kelleher JK, Stephanopoulos G. Elementary metabolite units (EMU): A novel framework for modeling isotopic distributions. Metab Eng 2007;9:68–86. doi:10.1016/j.ymben.2006.09.001.
[42] Antoniewicz MR, Kelleher JK, Stephanopoulos G. Determination of confidence intervals of metabolic fluxes estimated from stable isotope measurements. Metab Eng 2006;8:324–37. doi:10.1016/j.ymben.2006.01.004.
[43] Droste P, Miebach S, Niedenführ S, Wiechert W, Nöh K. Visualizing multi-omics data in metabolic networks with the software Omix—A case study. Biosystems 2011;105:154–61. doi:10.1016/j.biosystems.2011.04.003.
[44] Pirt SJ. Maintenance energy: a general model for energy-limited and energy-sufficient growth. Arch Microbiol 1982;133:300–2. doi:10.1007/BF00521294.
[45] Stephanopoulos GN, Aristidou AA, Nielsen J. Review of Cellular Metabolism. Metab. Eng., San Diego: Academic Press; 1998, p. 21–79. doi:10.1016/B978-012666260-3/50003-0.
[46] Taccari M, Canonico L, Comitini F, Mannazzu I, Ciani M. Screening of yeasts for growth on crude glycerol and optimization of biomass production. Bioresour Technol 2012;110:488–95. doi:10.1016/j.biortech.2012.01.109.
[47] Fiaux J, Cakar ZP, Sonderegger M, Wuthrich K, Szyperski T, Sauer U. Metabolic-Flux Profiling of the Yeasts *Saccharomyces cerevisiae* and *Pichia stipitis*. Eukaryot Cell 2003;2:170–80. doi:10.1128/EC.2.1.170-180.2003.
[48] Gancedo JM. Yeast carbon catabolite repression. Microbiol Mol Biol Rev 1998;62:334–61.
[49] Jordà J, Rojas H, Carnicer M, Wahl A, Ferrer P, Albiol J. Quantitative Metabolomics and Instationary 13C-Metabolic Flux Analysis Reveals Impact of Recombinant Protein Production on Trehalose and Energy Metabolism in *Pichia pastoris*. Metabolites 2014;4:281–99. doi:10.3390/metabo4020281.
[50] Nocon J, Steiger MG, Pfeffer M, Sohn SB, Kim TY, Maurer M, et al. Model based engineering of *Pichia pastoris* central metabolism enhances recombinant protein production. Metab Eng 2014;24:129–38. doi:10.1016/j.ymben.2014.05.011.
[51] Heyland J, Fu J, Blank LM, Schmid A. Quantitative physiology of *Pichia pastoris* during glucose-limited high-cell density fed-batch cultivation for recombinant protein production. Biotechnol Bioeng 2010;107:357–68. doi:10.1002/bit.22836.
[52] Celik E, Calik P, Oliver SG. Metabolic flux analysis for recombinant protein production by *Pichia pastoris* using dual carbon sources: Effects of methanol feeding rate. Biotechnol Bioeng 2010;105:317–29. doi:10.1002/bit.22543.
[53] Jordà J, Suarez C, Carnicer M, ten Pierick A, Heijnen JJ, van Gulik W, et al. Glucose-methanol co-utilization in *Pichia pastoris* studied by metabolomics and instationary 13C flux analysis. BMC Syst Biol 2013;7:17. doi:10.1186/1752-0509-7-17.
[54] Bakker BM, Overkamp KM, van Maris AJ, Kötter P, Luttik MAH, van Dijken JP, et al. Stoichiometry and compartmentation of NADH metabolism in *Saccharomyces cerevisiae*. FEMS Microbiol Rev 2001;25:15–37. doi:10.1111/j.1574-6976.2001.tb00570.x.
[55] Kyle M, Acharya K, Weider LJ, Looper K, Elser JJ. Coupling of growth rate and body stoichiometry in *Daphnia*: a role for maintenance processes? Freshw Biol 2006;51:2087–95. doi:10.1111/j.1365-2427.2006.01639.x.
[56] Elser JJ, Acharya K, Kyle M, Cotner J, Makino W, Markow T, et al. Growth rate-stoichiometry couplings in diverse biota. Ecol Lett 2003;6:936–43. doi:10.1046/j.1461-0248.2003.00518.x.
[57] Franklin O, Hall EK, Kaiser C, Battin TJ, Richter A. Optimization of biomass composition explains microbial growth-stoichiometry relationships. Am Nat 2011;177:E29--42. doi:10.1086/657684.
[58] Blank LM, Lehmbeck F, Sauer U. Metabolic-flux and network analysis in fourteen hemiascomycetous yeasts. FEMS Yeast Res 2005;5:545–58. doi:10.1016/j.femsyr.2004.09.008.

Figure Captions

Table 1. Reconciled macroscopic growth parameters for glycerol cultivations at different growth rates. D_{SP} (h^{-1}) corresponds to the set point dilution rate and D_{exp} (h^{-1}) to the

654 experimentally measured D. q_S, q_{O_2} and q_{CO_2} are expressed in mmol · g_{DCW}^{-1}· h^{-1}. Units for q_X are Cmmol · g_{DCW}^{-1}· h^{-1}.Y_{XS} represents biomass yield ($g_X \cdot g_S^{-1}$). RQ is the respiratory quotient.

656 **Table 2. Main properties of *P. pastoris* models used and generated in this study.**

657 **Fig. 1. Metabolic flux distribution estimated for *P. pastoris* growing on glycerol at**
658 **different dilution rates**. 0.05 h^{-1} (top box), 0.10 h^{-1} (middle box) and 0.16 h^{-1} (bottom box).
659 Results are expressed as the 95% confidence interval of the estimated fluxes relative to the
660 glycerol uptake rate in mmol glycerol · g_{DCW}^{-1} · h^{-1}. Lower and upper bounds of CI correspond to
661 the maximum and minimum CI bounds between the replicates. Flux directionality assumption
662 was represented by arrows; therefore, negative fluxes describe opposite direction.
663

664 **Table 1**

D_{SP}	0.05	0.10	0.16
D_{exp}	0.046 ± 0.006	0.098 ± 0.009	0.166 ± 0.006
q_S	-0.72 ± 0.11	-1.45 ± 0.13	-2.52 ± 0.14
q_X	1.62 ± 0.21	3.43 ± 0.31	5.89 ± 0.23
q_{CO_2}	0.55 ± 0.12	0.93 ± 0.07	1.65 ± 0.18
q_{O_2}	-0.90 ± 0.18	-1.66 ± 0.14	-2.89 ± 0.25
Y_{XS}	0.70 ± 0.02	0.73 ± 0.01	0.72 ± 0.01
RQ	0.60 ± 0.02	0.56 ± 0.01	0.57 ± 0.01

665

666

667 **Table 2**

	iMT1026 v3.0	*PpaPruned*	*PpaCore*	Openflux *PpaCore*
# reactions	2237	495	77	120
# internal metabolites	1706	513	102	100
# external metabolites	175	9	9	9
Maximal biomass generation rate ($g \cdot gDCW^{-1} \cdot h^{-1}$)	0.0940	0.0939	0.0939	-

675 **Fig. 1**

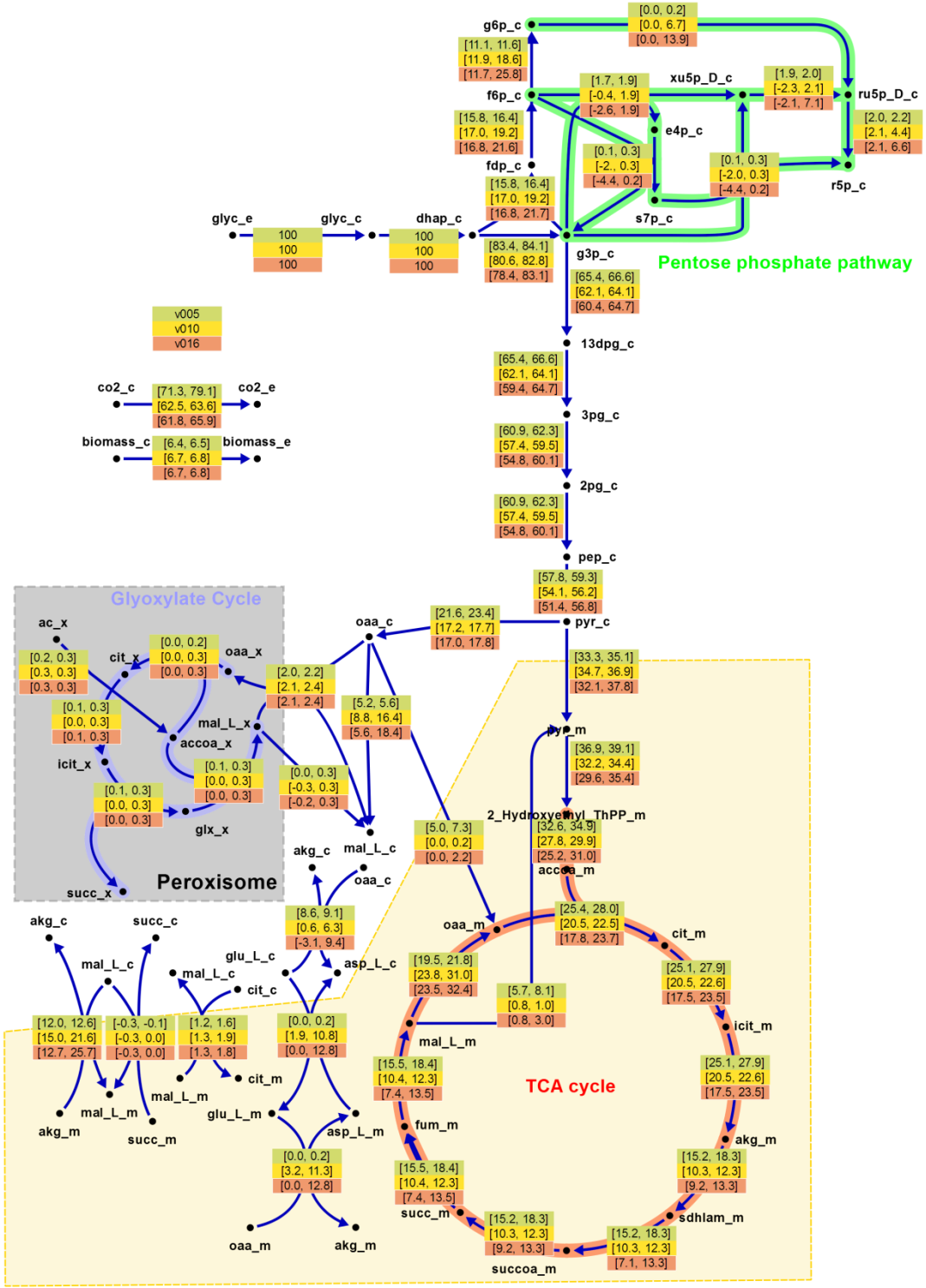

676

677

678

Additional File S1. Contains the original (*PpaGS*), reduced (*PpaPruned*) and compressed model (*PpaCore*) in Cell Net Analyzer format. In addition, the instructions followed for generating the reduced model are also included and described. *PpaGS* model is derived from the original iMT1026 v3.0, but due to numerical tolerance constrains in model reduction, the 'cof_c' metabolite was removed from the specific biomass equation describing growth on glycerol.

Additional File S2. Contains: **Table S1**: The Reduced stoichiometric model used for 13C-MFA. **Table S2**: Corrected experimental and simulated MIDs for each experimental replicate and corresponding analysed peaks from each corresponding derivatisation method. **Table S3:** Metabolic flux distribution estimated for *P. pastoris* growing on glycerol at different dilution rates. **Fig. S1**: Correlation among the calculated ATP turnover and the corresponding growth rate.